DOI 10.1007/s10946-024-10199-1
*Journal of Russian Laser Research, Volume 45, Number 2, March, 2024*

# MAX PHASE CHROMIUM–TITANIUM–ALUMINUM CARBIDE FOR ULTRAFAST LASER GENERATION IN THE 1.55 μm RANGE

**Ahmed Shakir Al-Hiti,* Noor Alhuda Mohammed, Mahmood Nabeel, and Nabaa Abdul Sattar**

*Department of Electrical Engineering, Faculty of Engineering, University of Anbar Anbar 31001, Iraq*

*Corresponding author e-mail: ahmed.s.abd@uoanbar.edu.iq

**Abstract**

We formally generate picosecond laser pulses in an Erbium-doped fiber laser (EDFL) by incorporating a new type of a saturable absorber (SA) with Chromium–Titanium–Aluminum carbide ($Cr_2TiAlC_2$). The SA film is prepared by a casting method, using polyvinyl alcohol (PVA) as a host. The novel ultrafast laser operates at 1559.96 nm; the laser pump power range is 164 – 305 mW. Using a 90 : 10 output coupler, the designed laser produces a pulse duration of 2.04 ps and a repetition rate of 1.855 MHz. We obtain a maximum output power of 3.2 mW and a pulse energy of 1.72 nJ at a maximum laser pump power of 305 mW. To the best of our knowledge, this is the first time that a $Cr_2TiAlC_2$-based SA is used to produce ultrashort laser pulses.

**Keywords:** $Cr_2TiAlC_2$, ultrafast laser, saturable absorber, Erbium-doped fiber.

## 1. Introduction

Mode-locked pulse lasers have been applied in several fields of scientific research such as the material science [1], medicine [2], and military applications [3]. Also, they have important characteristics, namely, the narrow pulse width [4], as well as the high pulse repetition rate [5] and high pulse energy [6]. One of the basic approaches to achieve passive mode locking is to use an optical component known as a saturable absorber (SA). The SA is introduced into the laser cavity to generate pulses in different infrared spectral ranges [7, 8].

The semiconductor saturable absorber mirrors (SESAMs) are among the most widely used and well-known SA mirrors in ultra-short pulse generation [9]. The SESAM has high stability, which makes it one of the best choices for SAs. In addition, the saturable intensity and recovery time are the exceptional properties of a SESAM, which are realized by modifying its structure [10]. However, the employment of the SESAMs as SAs has become limited due to their ultra-narrowband operation, low damage threshold, and complex manufacturing process [11]. Carbon nanotubes (CNTs) have gained prominence in novel electronics and photonic applications, due to their unique features [12, 13]. The CNT SA thin film showed better performance than SESAMs in ultra-short pulse generation applications [14]. However, CNTs suffer from issues associated with the nanotube diameter, which affects the operation bandwidth, band gap, and absorption efficiency [15, 16]. Two-dimensional (2D) atomic-layer-thick materials, which can be one layer or several layers within the thin-film SA, have also been considered [17]. Several unique electrical and optical elements have been demonstrated with their properties governed by the

Manuscript submitted by the authors in English on January 11, 2024.

 1071-2836/24/4502-0162

geometrical structure between the layers of the material, which includes graphene [18], transition metal dichalcogenides (TMD) [19, 20], and black Phosphorus (BP) [21]. These materials have been applied in the fiber lasers and showed fast recovery time and a broad spectral range [22]. But they have low modulation depth and a narrow band gap (between 0 and 1.5 eV) [17, 23, 24].

Recently, MAX phase materials have attracted many researchers due to their unique metallic and ceramic properties [25–27]. The MAX phase can be formulated as $Mn_{+1}AX_n$, with M being a transition metal, A being some element (such as Aluminum or silicon), and $X$ being carbon or Nitrogen [28]. They also have advantages of damage tolerance, thermal shock resistance, high electrical conductivity, and machinability. Therefore, they have been used in various fields, including high-temperature nuclear engineering applications [29, 30]. Chromium–Titanium–Aluminum carbide ($Cr_2TiAlC_2$) is a MAX phase material, with the physical properties similar to those of metallic and ceramic materials. $Cr_2TiAlC_2$ has been widely employed in various industrial applications, due to its unique properties such as thermal stability [31] and oxidation resistance [32]. In this study, we demonstrate ultra-short pulse generation, employing $Cr_2TiAlC_2$ as an SA in the 1.55 μm range. The SA is prepared via the drop-casting approach. It provides generation of stable mode-locked pulses with operation at 1556.96 nm, the 1.855 MHz repetition rate and the 2.04 ps pulse duration. Compared with other reported SAs, the new SA material has a very high damage threshold of more than 305 mW, with simpler and facile fabrication. It is also cheap and has great durability at high temperatures.

## 2. Fabrication and Characterization of $Cr_2TiAlC_2$ PVA

The SA film is fabricated, using the drop-casting method. The preparation process of the $Cr_2TiAlC_2$ PVA SA is simple and of low cost. Initially, 1 g of polyvinyl alcohol (PVA) is poured into 100 ml of deionized (DI) water with stirring by a magnetic stirrer at 500 rpm for 120 min. at room temperature. Meanwhile, 10 mg of a $Cr_2TiAlC_2$ powder is dropped into 15 ml of the prepared PVA solution. The $Cr_2TiAlC_2$/PVA solution is stirred at 500 rpm for 4 h. at room temperature. Then, the mixture solution is dropped into a Petri dish to dry at room temperature for 72 h. to form a $Cr_2TiAlC_2$ PVA film. After 72 h., the SA film is cut into a small piece 1×1 mm in size, attached to a clean FC/PC fiber ferrule with an index matching gel, and placed into the laser cavity.

In Fig. 1, we show the nonlinear optical absorption characteristics of the $Cr_2TiAlC_2$-based SA. In Fig. 1 a, we present the nonlinear optical absorption setup of the $Cr_2TiAlC_2$ SA, using a balanced double-detector measurement configuration. It consists of an ultrafast laser source operating at 1556.96 nm, with a pulse width of 2.04 ps and a repetition rate of 1.855 MHz, used as the input pulsed laser source. An Erbium-doped fiber amplifier (EDFA: OPA-1550S-27) amplifies the mode-locked laser to the variable optical attenuator. Then, a coupler (50 : 50) is employed to split the laser beam and evaluate the performance. The results are fitted by the saturation model formula

$$T = 1 - \Delta T/(1 + I/I_{\text{sat}}) - \alpha_{\text{ns}}, \tag{1}$$

where $\Delta T$ is the modulation of transmittance by saturable absorption, $I$ is the input intensity, $I_{\text{sat}}$ is the saturation intensity, $T$ is the transmission coefficient, and $\alpha_{ns}$ is the non-saturable absorption.

The saturable absorption, saturation intensity, and non-saturable absorption of the proposed SA film are estimated to be 10%, 0.06 mW/cm$^2$, and 20%, respectively; see Fig. 1 b. The proposed SA film achieves acceptable results that can be compared with other materials.

The scanning electron microscope (SEM) image of $Cr_2TiAlC_2$ PVA is given in Fig. 2 a. The SEM image of the SA film demonstrates a uniform distribution of $Cr_2TiAlC_2$ particles in the PVA polymer within 2 μm. It also shows large particles believed to be $Cr_2TiAlC_2$. In Fig. 2 b, we show the $X$-ray diffraction (XRD) analysis of the $Cr_2TiAlC_2$ thin film. Different peaks appear in the XRD pattern measured within the range of degrees from 10° to 70°. The first peak appears at 19.5°, which represents the establishment of a crystalline structure of polyvinyl alcohol in the $Cr_2TiAlC_2$ PVA film [33].

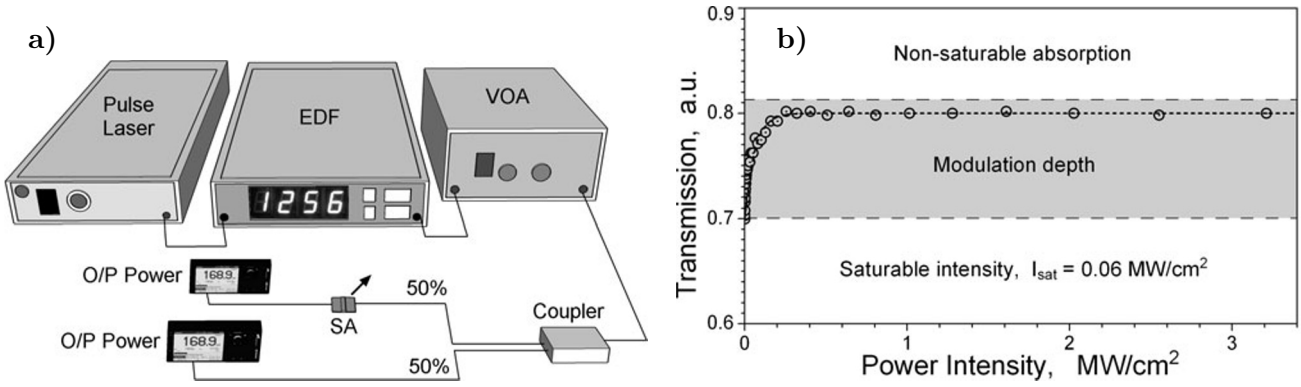


**Fig. 1.** The linear and nonlinear characteristics of $Cr_2TiAlC_2$ PVA; here, nonlinear absorption measurement configuration (a) and nonlinear absorption (b), where ⊙ shows an experimental data and short-dashed curve shows the modulation fit.

Other peaks are recorded at 10.11°, 20.09°, 29.99°, 36.16°, 39.31°, 41.20°, 43.01°, 44.64°, 50.81°, 55.22°, 59.56°, and 64.30°, which correspond to the (002), (004), (005), (006), (007), (009), (0010), (017), (018), (019), and (110) crystalline planes, respectively. These are obtained due to the increasing contribution of TiC and $Cr_2AlC$ with increasing temperature, using the PVA polymer.

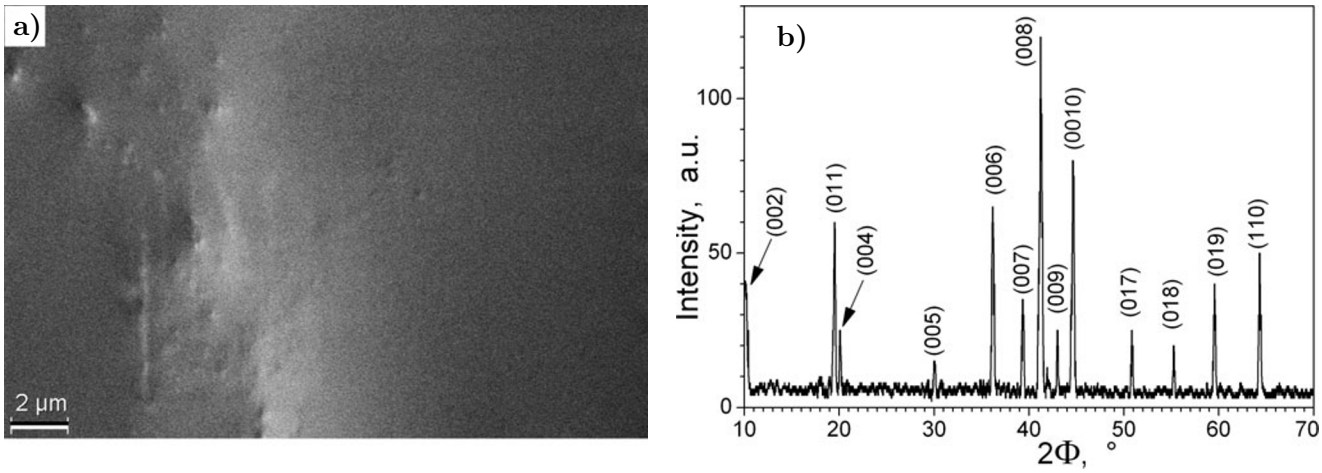


**Fig. 2.** The $Cr_2TiAlC_2$ PVA film characterization; here, SEM image (a) and XRD analysis of $Cr_2TiAlC_2$ PVA (b).

## 3. Laser Configuration

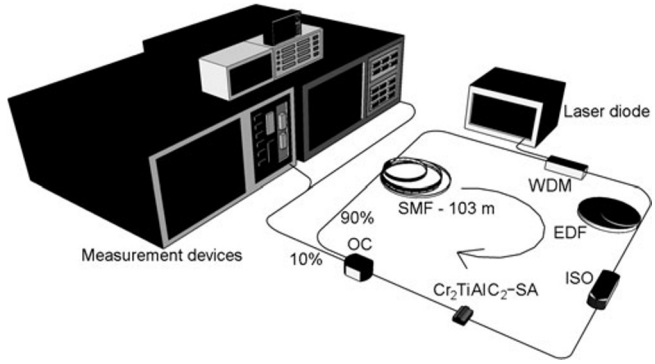


**Fig. 3.** Laser setup of ultrafast operation, using $Cr_2TiAlC_2$ PVA as the SA.

In this paper, we demonstrate an ultrafast laser, using a $Cr_2TiAlC_2$-based SA. The total cavity length is 111.5 m. The experimental setup contains a laser diode (LD), wavelength division multiplexer (WDM), and a 103 m long single-mode fiber (SMF), with a 2 m Erbium-doped fiber (EDF) used as the gain medium. The EDF has the 0.16 numerical aperture, 125 μm cladding diameter, 4 μm core diameter, and 23 dB/m Erbium ion concentration. The experimental setup for the mode-locked laser is shown in Fig. 3. The ring cavity has a 980 nm LD source pumping through the 980/1550 WDM. An isolator (ISO) is utilized to ensure unidirectional laser beam propagation in the cavity. A 90 : 10 output coupler (OC) is introduced in the laser cavity to extract 10% of the beam power to monitor the laser performance. An OSA (Anritsu, MS 9710C optical spectrum analyzer) with a resolution of 0.2 nm, an oscilloscope (GWINSTEK, GSP-9300B), a radio-frequency spectrum analyzer (RFSA, Anritsu, MS 2803A), and an OPM (Thorlabs, PM100D, optical power meter) are used to analyze the laser power and output spectrum.

## 4. Mode-Locked EDFL Performance

Initially, a continuous-wave (CW) emission is produced at a 10 mW input power. A stable ultra-short pulse is obtained at the pump power in the range of 164 to 305 mW. In Fig. 4 a, we show the pulse train for the mode-locked operation at a maximum laser pump power of 305 mW. The pulse train is uniform with a pulse rate of 1.855 MHz and a pulse width of 33.77 ns. When the laser pump power is increased above 305 mW, the ultrafast laser pulses vanish, and no pulses are detected in the oscilloscope trace. Thus, the soliton shape is shifted to a single wavelength centered at 1556 nm, due to oversaturation of the SA in the laser cavity [34]. As the laser pump power is again reduced below 305 mW, ultra-short pulses are reproduced. This demonstrates that the optical damage threshold of the designed SA is higher than 305 mW. In Fig. 4 b, we show two stable pulses having a pulse rate of 1.855 MHz and a pulse period of 539 ns.

The output spectrum of the mode-locked EDF laser is obtained via the OSA trace; see Fig. 4 c. The mode-locked laser spectrum is centered at a wavelength of 1556.96 nm, with a 3 dB bandwidth of 1.52 nm. The sub-sidebands of soliton pulses are obtained with a cavity length of 111.5 m. The soliton sub-sidebands appear strong despite the use of the long cavity, due to the low insertion loss of our SA, which maintains a high fractional strength [35]. The pulse width determined by the oscilloscope trace is 33.77 ns. This is not the real value due to the resolution limitations. Therefore, we use an autocorrelation device (Alnair Labs. Hac-200) to measure the actual pulse, which appears to be about 2.04 ps; see Fig. 4 d. We estimate the time–bandwidth product (TBP) to be 0.383, which is close to the transform-limited TBP for $\text{sech}^2$ pulses of 0.315.

In Fig. 5 a, we illustrate the radio-frequency (RF) spectrum of the mode-locked EDF laser. The RF spectrum is acquired at a maximum pump power of 305 mW with a range of 39.5 MHz, which corresponds to a pulse rate of 1.855 MHz. A single-to-noise ratio (SNR) of 57 dB is achieved, indicating the high

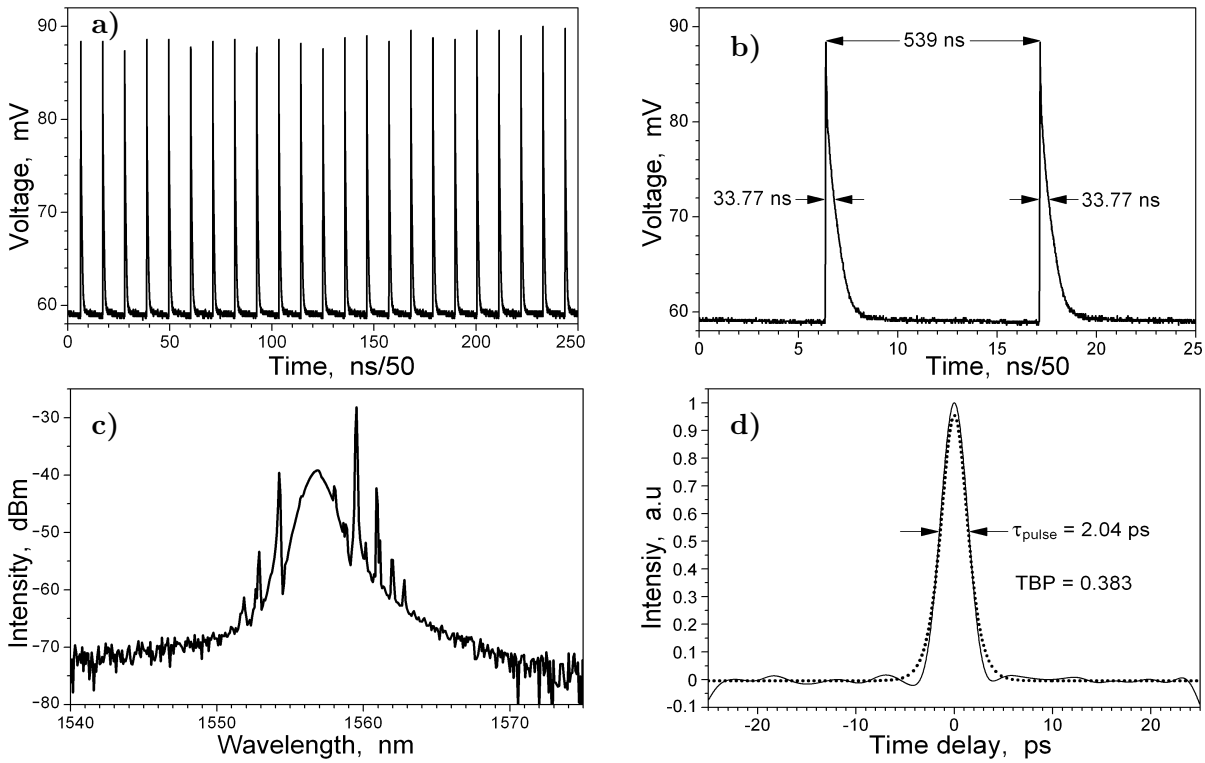


**Fig. 4.** The oscilloscope trace, laser wavelength, and autocorrelator measurement result; here, the pulse train (a), two pulse envelopes (b), the laser wavelength (c), and actual pulse width (d).

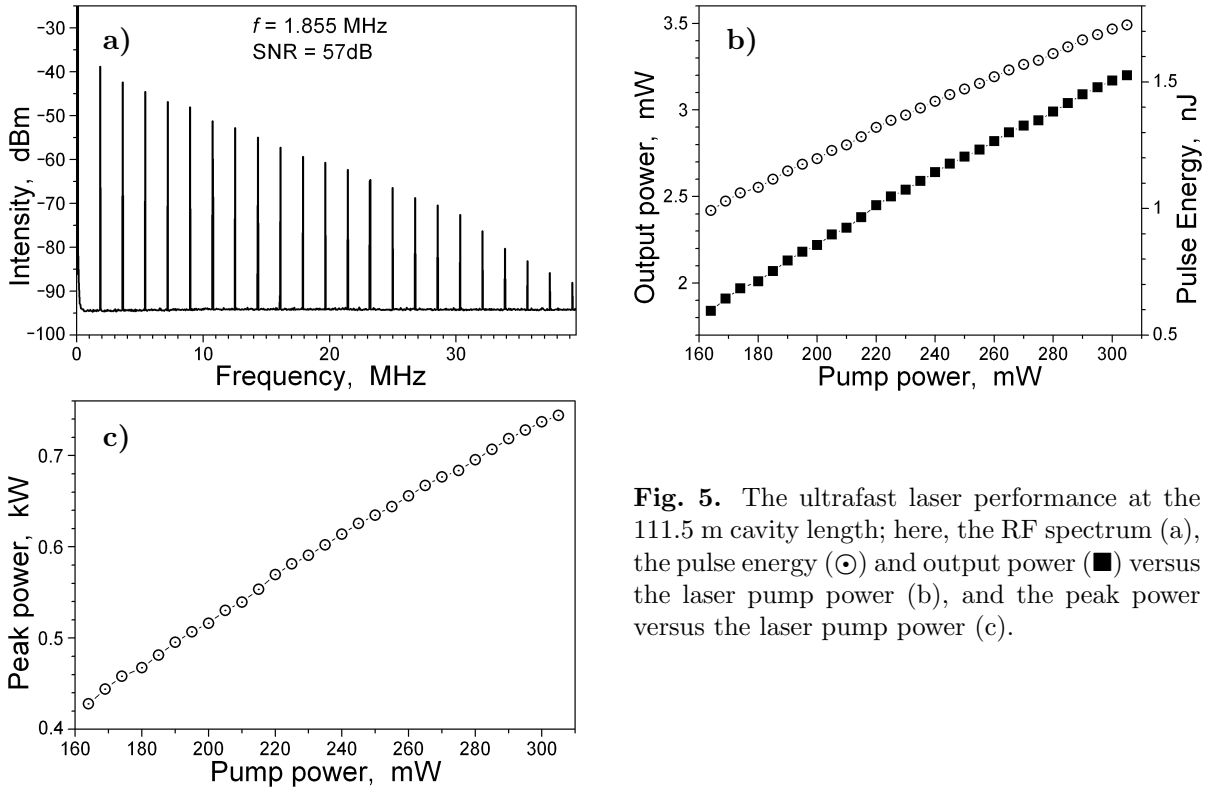


**Fig. 5.** The ultrafast laser performance at the 111.5 m cavity length; here, the RF spectrum (a), the pulse energy (⊙) and output power (■) versus the laser pump power (b), and the peak power versus the laser pump power (c).

stability of the proposed laser setup. The pulse energy and average output power are obtained versus the input power; see Fig. 5 b. The maximum achieved pulse energy and output power are 1.72 nJ and 3.2 mW, respectively. In Fig. 5 c, we show the peak power versus the input power. The obtained peak power is from 0.42 to 0.74 kW.

## 5. Summary

In this paper, we demonstrated $Cr_2TiAlC_2$ PVA as the SA to achieve mode-locked EDFL operation. The mode-locked EDFL had a maximum repetition rate of 1.855 MHz and a minimum pulse width of 2.04 ps, with a maximum pulse energy of 1.72 nJ. The achieved saturation intensity and modulation depth were 0.06 mW/cm$^2$ and 10%, respectively. The MAX phase SA showed very good results with a passive mode-locker being in the 1.5 μm range.

## References


1. A. Nassiri and H. Idrissi-Saba, "High power and high energy seven-core ytterbium doped fiber laser for mateials processing application," 2017 International Conference on Engineering & MIS (ICEMIS), Monastir, Tunisia (2017); DOI: 10.1109/ICEMIS.2017.8273077
2. K. Al Hallak, S. Tomi, and D. Omran, *J. Cosmet. Laser Ther.*, **23**, 19 (2021).
3. S. Wang, X. Lin, Z. Zhang, et al., *Appl. Opt.*, **60**, 1117 (2021).
4. A. S. Al-Hiti, R. Apsari, M. Yasin, and S. W. Harun, *Infrared Phys. Tech.*, **116**, 103788 (2021).
5. M. M. Najm, S. W. Harun, S. Salam, et al., *Opt. Fiber Technol.*, **61**, 102439 (2021).
6. S. Li, Y. Yin, Q. Ouyang, et al., *Opt. Express*, **27**, 19843 (2019).
7. A. S. Al-Hiti, M. Yasin, and S. W. Harun, *Appl. Opt.*, **61**, 1292 (2022).
8. A. S. Al-Hiti, A. H. H. Al-Masoodi, M. M. Najm, et al., *Optik*, **231**, 166377 (2021).
9. U. Keller, K. J. Weingarten, F. X. Kartner, et al., *IEEE J. Sel. Top. Quantum Electron.*, **2**, 435 (1996).
10. U. Keller, *Nature*, **424**, 831 (2003).
11. A. S. Al-Hiti, A. H. H. Al-Masoodi, S. W. Harun, et al., *Opt. Laser Technol.*, **131**, 106429 (2020).
12. S. Yamashita, *J. Lightw. Technol.*, **30**, 427 (2011).
13. V. Scardaci, A. Rozhin, P. Tan, et al., *Phys. Status Sol. B*, **244**, 4303 (2007).
14. C.-H. Cheng and G.-R. Lin, *Curr. Nanosci.*, **16**, 441 (2020).
15. A. S. Al-Hiti, A. H. H. Al-Masoodi, W. R. Wong, et al., *Opt. Laser Technol.*, **139**, 106971 (2021).
16. M. Chernysheva, A. Rozhin, Y. Fedotov, et al., *Nanophotonics*, **6**, 1 (2017).
17. Q. Bao, H. Zhang, Y. Wang, et al., *Adv. Funct. Mater.*, **19**, 3077 (2009).
18. H. Zhang, D. Tang, L. Zhao, et al., *Opt. Express*, **17**, 17630 (2009).
19. Y. Yang, S. Yang, C. Li, and X. Lin, *Opt. Laser Technol.*, **111**, 571 (2019).
20. K. Niu, R. Sun, Q. Chen, et al., *Photonics Res.*, **6**, 72 (2018).
21. E. Ismail, N. Kadir, A. Latiff, et al., *RSC Adv.*, **6**, 72692 (2016).
22. C. Ma, C. Wang, B. Gao, et al., *Appl. Phys. Rev.*, **6**, 041304 (2019).
23. B. Chen, X. Zhang, K. Wu, et al., *Opt. Express*, **23**, 26723 (2015).
24. M. Zhang, Q. Wu, F. Zhang, et al., *Adv. Opt. Mater.*, **7**, 1800224 (2019).
25. M. W. Barsoum, *Prog. Solid. State Ch.*, **28**, 201 (2000).
26. Z. M. Sun, *Int. Mater. Rev.*, **56**, 143 (2011).
27. M. Xue, X. Zhang, H. Tang, and C. Li, *RSC Adv.*, **4**, 39280 (2014).
28. S. Li, W. Yu, H. Zhai, et al., *J. Eur. Ceram. Soc.*, **31**, 217 (2011).
29. S. P. Munagala, "MAX phases: New class of carbides and nitrides for aerospace structural applications,"

in: N. Eswara Prasad and R. J. H. Wanhill (Eds.), *Aerospace Materials and Material Technologies*, Vol. 1, *Aerospace Materials*, Springer, Singapore (2017), pp. 455-465; DOI: 10.1007/978-981-10-2134-3_20
30. G. M. Song, "Self-healing of MAX phase ceramics for high temperature applications: Evidence from $Ti_3AlC_2$," in: I. M. Low (Ed.), *Advances in Science and Technology of $M_{n+1}AX_n$ Phases*, Woodhead Publishing (2012), pp. 271-288; DOI: 10.1533/9780857096012.271
31. Z. Liu, J. Yang, H. Zhang, et al., *Ceram. Int.*, **49**, 12034 (2023).
32. Z. Liu, J. Yang, Y. Qian, et al., *Corros. Sci.*, **183**, 109317 (2021).
33. K. Nakane, T. Yamashita, K. Iwakura, and F. Suzuki, *J. Appl. Polym. Sci.*, **74**, 133 (1999).
34. H. Ahmad, M. Z. Samion, A. Muhamad, et al., *Laser Phys.*, **27**, 065110 (2017).
35. A. S. Al-Hiti, Z. C. Tiu, M. Yasin, and S. W. Harun, *Sci. Rep.*, **12**, 13288 (2022).